Spin waves in antiferromagnetic thin films and multilayers: Surface and interface exchange and entire-cell effective-medium theory

R. L. Stamps* and R. E. Camley†
Department of Physics, University of Essex, Colchester, Essex, CO4 3SQ, United Kingdom
(Received 15 April 1996; revised manuscript received 29 July 1996)

High-quality, insulating antiferromagnetic thin films and multilayers offer possibilities for new studies of exchange mechanisms at surfaces and across interfaces between dissimilar magnetic materials. Using a microscopic theory, we study long-wavelength spin waves to answer two questions: (1) Can we determine accurate values for surface and interface exchange from spin-wave frequencies and (2) can we obtain an effective-medium description which properly reproduces *all* the spin-wave excitations of the antiferromagnetic structure. We find that the frequencies of surface and interface modes are particularly sensitive to interface exchange values, even when the spin-wave frequencies for the two materials are far apart and little coupling is expected. We also present a method for calculating the dynamic magnetic response of a superlattice structure that avoids a serious approximation made in conventional effective-medium theory. Our effective-medium formulation gives results in excellent agreement with microscopic calculations and will be useful for characterizing thin antiferromagnetic films as well as large multilayers. Susceptibilities are derived which can be directly applied to calculations for infrared reflectivity experiments. [S0163-1829(96)03642-9]

I. INTRODUCTION

Up to now, the determination of exchange interactions at the interfaces of multilayers constructed from antiferromagnetic materials has only been accomplished by studying critical temperatures found from heat-capacity measurements.[1,2] Such measurements only provide estimates of the magnitude of the exchange integrals, with an accuracy no better than 50%.[2] Information regarding effective interfilm exchange obtained from other techniques is therefore of interest. This is especially relevant in light of the high-quality antiferromagnetic thin films and multilayers currently available.[3–6] For example, a recent study of ultrathin NiO films shows a structure with a well defined number of magnetic planes, and with finite-size effects determining thermal phase transitions.[7]

A useful approach for determining the magnitude and sign of effective interfacial exchange in other systems, such as metallic Fe/Cr/Fe multilayers, has involved sensitive measurements of shifts in the frequencies of long-wavelength spin waves.[8–11] In this paper we discuss how the same idea can be applied to investigate interfilm exchange in insulating multilayered antiferromagnets. Our study is in part motivated by recent advances in the measurement of spin-wave frequencies in antiferromagnets using infrared techniques,[12–14] and reports of standing spin waves in antiferromagnets.[15]

Multilayers constructed from different antiferromagnetic materials can be expected to show large effects of interfilm coupling on spin-wave frequencies if the magnetic resonance frequencies of each material are nearly degenerate.[16] If the response frequencies are similar, then interfilm coupling allows for hybridization between spin-wave modes with significant shifts of the frequencies away from their bulk material values. On the other hand, some of the more interesting multilayers are constructed from antiferromagnets with very dissimilar properties. These include FeF_2/MnF_2 (Ref. 4) and NiO/CoO (Ref. 17) superlattices where the spin-wave frequencies of the two antiferromagnets are far apart. The question then arises whether any appreciable effects on the spin-wave manifold due to interfilm exchange coupling can be expected at all.

Our results indicate that very dramatic effects of interfilm coupling can in fact be observed on *some* of the spin-wave modes in an antiferromagnetic multilayer. We also show how these effects can be detected by measuring infrared reflectivities.

Existing work on antiferromagnetic multilayers has primarily considered long-wavelength[18] approximations or microscopic[16,19] periodic superlattices. We approach the problem for finite structures using a microscopic theory applicable in both the long- and short-wavelength regions by properly including exchange and dipolar interactions.[20] This allows us to critically examine long-wavelength ''effective-medium'' approximations needed for discussing realistic large structures.[21–24] Our results show that conventional effective-medium theories are inadequate to properly describe the effects of interfilm exchange. We present an extended effective-medium theory that accurately describes interfilm exchange effects. Susceptibilities based on the modified effective-medium theory include contributions from standing spin-wave excitations that can have an important impact on reflectivities in thin-film structures. This kind of interesting and informative fine structure is missed by conventional effective-medium theory.

The paper is organized as follows. General theoretical considerations and the microscopic theory with results for thin films are discussed in Sec. II. The effects of interfilm exchange on spin-wave modes in multilayers are investigated in Sec. III using the microscopic formalism. Finally, a modified effective-medium theory is presented in Sec. IV and compared to results from the microscopic theory. Results for susceptibilities useful for calculating infrared optical response are also given. The work is summarized in Sec. V.

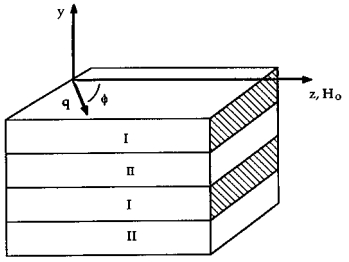

FIG. 1. Geometry. The magnetizations lie along the z axis and an external applied field is in the $+z$ direction. The in-plane wave vector $\mathbf{q}$ makes an angle ϕ with the z axis. The multilayer is constructed from two different antiferromagnetic films I and II. The axis of the multilayer is along the y direction.

II. FINITE-SIZE EFFECTS AND ANTIFERROMAGNETIC FILMS

A natural starting point for a discussion of collective spin-wave modes in multilayers is the analysis of spin waves in single films. Despite existing work on antiferromagnets and antiferromagneticlike multilayer structures, there are aspects of thickness dependence for spin waves in thin antiferromagnetic films that have not been addressed. We therefore first discuss relevant properties of spin waves in thin, easy-plane antiferromagnetic films as background for our critique of effective-medium theory in Sec. IV.

We begin by outlining the general theory for spin-wave excitations below, and then discuss calculated results for spin-wave propagation in thin, easy-plane antiferromagnetic films. The effects of interfilm coupling are described in Sec. III where we consider spin waves in a system of two coupled antiferromagnetic films, and in multilayers consisting of several antiferromagnetic films.

Equations of motion

The geometry is shown in Fig. 1. The individual films are composed of either material I or material II. Each material is a two sublattice antiferromagnet with antiparallel sublattices parallel to the plane of the films. The equilibrium direction of the magnetizations are assumed to be in-plane.

The wave vector of a spin excitation is given by $\mathbf{q}$ and a static magnetic field is applied in the z direction. The y direction is normal to the films and the multilayer consists of N pairs of magnetic sublattices. The general Hamiltonian for both the microscopic theory and the effective-medium approximations discussed later in this paper is

$$H=\sum_{\langle i,j\rangle} J(i,j)\mathbf{S}(i)\cdot\mathbf{S}(j) - \sum_{i} [g\mu_B H_o S_z(i)+K_a(i)S_z(i)^2+K_u(i)S_y(i)^2] + \sum_{i\neq j} \mathbf{D}(i,j)\mathbf{S}(i)\cdot\mathbf{S}(j). \quad (1)$$

The indices i and j identify lattice sites, and the brackets $\langle i,j\rangle$ denote a sum over nearest neighbors. The first term describes exchange coupling between nearest neighbors with magnitude J. The second set of terms are applied field, out-of-plane, and in-plane anisotropies, represented by H_o, K_a, and K_u, respectively. The last term is the long-range dipole interaction governed by the matrix $\mathbf{D}$. The spin operators $\mathbf{S}(i)$ are assumed to be localized to each lattice site.

We assume that the films are periodic in-plane and use translational invariance in order to expand all position dependent variables in Fourier series in the the x and z directions. The wave vector $\mathbf{q}$ governs the spatial variation in the Fourier expansion. A simple cubic structure with lattice spacing a is assumed for simplicity and throughout the paper we use the index n to identify the atomic layer number. The calculation of spin-wave frequencies consists of solving linearized equations of motion derived from the above Hamiltonian in the long-wavelength limit. These are of the form

$$-i\hbar\omega\mathbf{s}_n=\mathbf{s}_n\times\{g\mu_B[\hat{\mathbf{z}}H_o+\mathbf{H}_n^s]+\hat{\mathbf{z}}H_a(n)+\hat{\mathbf{y}}H_u(n) + 4J_{n,n}\mathbf{S}_n+J_{n,n-1}\mathbf{S}_{n-1}+J_{n,n+1}\mathbf{S}_{n+1}\} + \mathbf{S}_n\times\{g\mu_B\mathbf{h}_n(\mathbf{q})+2J\mathbf{s}_n[\cos q_x a+\cos q_z a] + J_{n,n-1}\mathbf{s}_{n-1}+J_{n,n+1}\mathbf{s}_{n+1}\}. \quad (2)$$

The notation uses $\mathbf{s}_n$ to represent time-dependent spin operators and $\mathbf{S}_n$ to represent static spin operators. These are treated as classical vectors in the long-wavelength limit. $\mathbf{H}_n^s$ are time-independent demagnetizing fields and $\mathbf{h}_n(\mathbf{q})$ are time and spatially varying demagnetizing fields. $J_{n,n-1}$ is the exchange interlayer coupling between layers n and $n-1$. For convenience, the equations of motion have been written in terms of effective anisotropy fields. These are defined as H_a for the in-plane anisotropy and H_u for the out-of-plane anisotropy. The effective anisotropy fields are defined in the usual way; i.e., an effective anisotropy field $H_{\rm ani}$ is $H_{\rm ani}=2K/M$, where K is an anisotropy energy such as K_a or K_u and M is a saturation magnetization for a sublattice.

For future reference, we introduce additional simplifying notation. First, we define effective exchange fields. The interlayer effective exchange field is defined as H_e, and the corresponding interfilm field acting across the interfaces in multilayers is $H_{\rm I}$. Both are defined using relations such as $H_e=2J/M$. Finally, the anisotropies and exchange fields are assumed uniform throughout the films, but are material dependent. We therefore drop explicit reference to layer number n and instead refer to the film material. Since we consider only two different antiferromagnetic materials in the multilayer, the associated parameters are identified in the remainder of the paper by the superscripts I and II, respectively.

Thickness dependence in thin antiferromagnetic films

An understanding of thickness dependence for spin-wave frequencies in thin films is necessary in order to understand collective spin-wave excitations in combinations of thin films. In this section we concentrate on aspects of thickness dependence for single thin antiferromagnetic films that do not appear in the existing literature. We illustrate below some features of spin-wave behavior in antiferromagnetic thin-film geometries using a microscopic theory based on Eqs. (1) and (2). As described in the introduction, this same microscopic theory will also be applied in order to judge the effective-medium theory presented later in this paper.

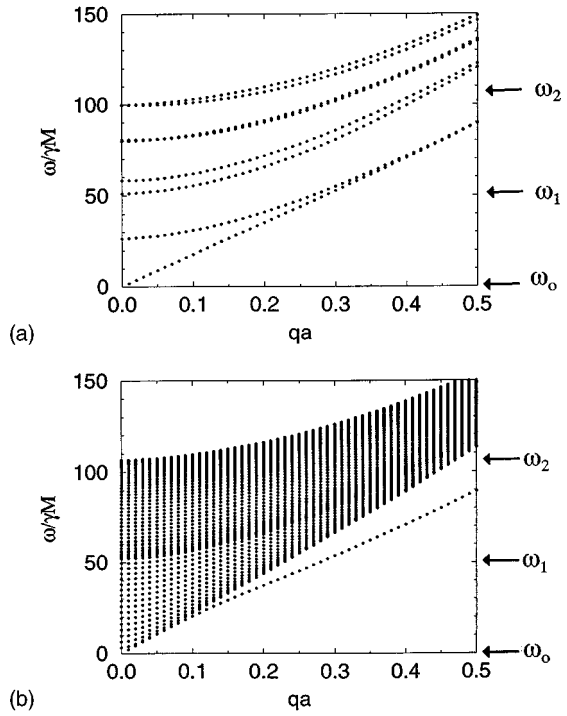

FIG. 2. Spin-wave frequencies as a function of wave vector **q** for a thin antiferromagnetic film of (a) 8 and (b) 48 atomic layers. The frequencies were calculated using the microscopic theory described in the text. There is no applied field and propagation is perpendicular to the magnetization. The film is easy plane with no in-plane anisotropy ($H_a=0$), $H_u/M=1$ and $H_e/M=100$. The spin-wave modes fall into two bands. At $q=0$ the lower limit frequencies are ω_0 and ω_1 and the upper limit frequency is ω_2. Here ω_0 is zero since we have taken $H_a=0$.

Because this theory includes both dipolar and exchange interactions in a microscopic model, it provides a useful way to demonstrate finite-size effects and the effects of interfilm exchange on spin-wave frequencies. These are topics which have not been completely dealt with in previous studies. The essence of the microscopic theory is described in Refs. 20 and 23, and involves directly solving Eqs. (2) using explicit sums for the dipole interaction terms.[25]

Results from this theory are given in Fig. 2 where the dependence of the frequencies on in-plane wave vector **q** for a single, thin, easy-plane antiferromagnetic film is shown. The frequencies were calculated for an eight-layer easy-plane antiferromagnetic film in (a) and a 48-layer film in (b). The parameters are $H_u/M=1$, $H_a/M=0$, and $H_e/M=100$. $H_o=0$ and propagation is perpendicular to the magnetization direction. Results are shown in unitless frequencies $\omega/\gamma M$ where $\gamma=g\mu_B/h$. Here and in the remainder of the paper, for simplicity M is the same for all sublattices and materials.

The limits ω_0 and ω_1 correspond to lower bulk band limits in an easy-plane antiferromagnet. These bands are nondegenerate even in the absence of an applied field. At $q=0$ the limits are given by

$$\omega_0=\gamma[H_a(2H_e+H_a+H_u+4\pi M)]^{1/2}, \tag{3}$$

$$\omega_1=\gamma[(2H_e+H_a)(H_a+H_u+4\pi M)]^{1/2}. \tag{4}$$

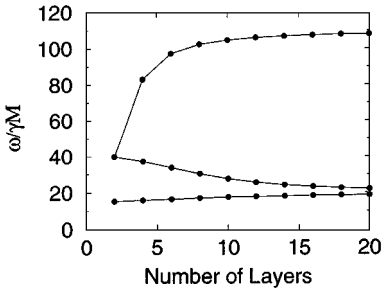

FIG. 3. Thickness dependence of spin-wave frequencies in an easy plane antiferromagnet. The applied field is $H_o/M=0.5$ and the parameters are $H_e/M=100$, $H_a/M=2$, $H_u/M=1$, and $\mathbf{q}=0$. The frequencies for the highest and lowest two spin-wave modes are shown for different film thicknesses. The two lowest frequency spin-wave modes are localized to the surfaces as the film thickness is increased.

These are a generalization of results presented in Ref. 23 to include two orthogonal uniaxial anisotropies.

We note that ω_1 is the usual antiferromagnetic resonance frequency including a shape anisotropy, $4\pi M$, due to the easy-plane configuration with sheets of parallel spins. Spin-wave excitations have frequencies that lie above ω_0 with energies determined by the wave vector of the mode. In a thin-film geometry, finite-size effects result in a quantization of the wave-vector component normal to the film plane. The lowest frequency mode in Fig. 2 is the resonance mode at $q=0$ and a surface mode for finite q and propagation perpendicular to the magnetization. The next highest frequency mode is also a surface mode at finite wave vectors.

The highest possible frequency at $q=0$ includes large exchange energy contributions corresponding to a rapidly oscillating standing wave in the y direction. The frequency, which we call ω_2, is

$$\omega_2=\gamma[(H_e+H_a)(H_e+H_a+H_u+4\pi M)]^{1/2}. \tag{5}$$

This frequency is also shown in Fig. 2 at $q=0$.

The effects of finite film thickness can be seen by comparing Figs. 2(a) and 2(b). Additional modes appear as the film is made thicker, thus forming a continuum of modes between the band limits. Note that the frequency of the modes at the top of the bands increase with film thickness.

The thickness dependence of the highest and two lowest frequency modes is shown in Fig. 3. The parameters are $H_e/M=100$, $H_a/M=2$, $H_u/M=1$, and $q=0$. The frequency shifts of all the modes are substantial. Even the lowest frequency spin wave, which is the mode least affected by film thickness, changes by about 10% for the thicknesses considered. The next highest and highest frequency modes show an even stronger dependence on film thickness.

The reason for these strong thickness dependences is the reduced coordination number for spins at the surfaces. This means that the effective average exchange field experienced by a spin at the surface is very different from that acting on a spin in the bulk. For thin films, this means that the surface exchange fields play a significant role in the frequencies of all modes. This is a result of an effective pinning condition introduced by the surface exchange field. As the film becomes thicker, the surface becomes a small perturbation to the spin wave's energy. Similar behavior will be shown to

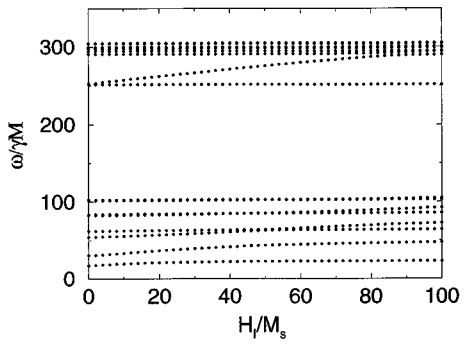

FIG. 4. Spin-wave frequencies as a function of interfilm exchange H_{I} for two coupled films. Each film has eight atomic layers. The exchange and out of plane anisotropies are the same in each film (with $H_e/M=100$ and $H_u/M=1$) but $H_a^{\mathrm{I}}/M=200$ and $H_a^{\mathrm{II}}/M=2$. The applied field is $H_o/M=0.5$ and $qa=0.002$. The surface modes are sensitive to H_{I} even though the bands corresponding to the two different films are well separated in frequency.

occur in multilayers where the interfilm coupling controls the impact of the interface exchange fields on spin-wave frequencies. Explicit examples of effective pinning in multilayer geometries are discussed in the next section.

III. INTERFILM EXCHANGE INDUCED FREQUENCY SHIFTS

In order to understand spin waves in multilayers, we first examine the simplest possible multilayer: two coupled antiferromagnetic films. Spin-wave frequencies for two exchange coupled films are shown in Fig. 4 as a function of the coupling between the films. The frequencies were found using the microscopic theory described above. Each film is eight atomic layers thick and the films are different antiferromagnets. Film I has $H_a^{\mathrm{I}}/M=200$ and film II has $H_a^{\mathrm{II}}/M=2$. For both films, $H_u/M=1$ and $H_e/M=100$. The applied field is $H_o/M=0.5$ and $qa=0.002$.

Two sets of modes are apparent, with limits corresponding to the different magnetic parameters of each film. Note that the lowest frequency modes associated with film II are surface modes and lie well below ω_0 for this film ($\omega_0/M=287$). A surface mode in each set increases in frequency with increasing H_{I} and crosses through the band of higher frequency modes. The result are a number of weak mode repulsions within each band that depend on the magnitude of H_{I} and the anisotropies.

We comment briefly on our range of values for the interfacial exchange field, H_{I}. Comparisons of theory and experiment on high-quality antiferromagnetic multilayers seem to indicate that H_{I} can be quite large, the same order of magnitude as the exchange field within an individual film. Clearly one could also construct antiferromagnetic superlattices with additional spacer layers between antiferromagnets so as to reduce this coupling. Thus the range we have chosen, $H_{\mathrm{I}}=0$ to $H_{\mathrm{I}}=H_e$, seems to appropriately cover this range.

In our example we have chosen antiferromagnets where there is a large gap between resonance frequencies for the two materials. This is not atypical. For example, a multilayer of alternating FeF_2 and MnF_2 films will have a gap of approximately 280 kG between the resonance modes of the films. This means that the spin-wave frequencies are very different for the two materials and hybridization effects due to interfilm exchange are small for most modes.

As we see in Fig. 4, however, some individual modes are nevertheless very sensitive to the interfilm exchange. The reason is that the coupling acts to control the degree to which spins at the interfaces are dynamically ''pinned.'' The pinning strongly modifies the component of the wave vector normal to the films and occurs because spins at the interfaces are driven at a frequency away from their natural resonance frequency. This off-resonance driving is controlled by the interfilm exchange.

Of all the spin waves, the surface modes are the most sensitive to pinning effects because they have the largest amplitude at the interfaces. This has an interesting consequence for conventional effective-medium theories. Effective-medium theory generally assumes long-wavelength excitations with amplitudes that vary slowly across the multilayer. Consequently there is no possibility for pinning of long-wavelength excitations in thin antiferromagnets. It is therefore not possible to accurately predict interfilm exchange caused frequency shifts using conventional effective-medium theory. In Sec. IV we describe how to construct an effective-medium theory capable of overcoming this limitation.

Additional insight into the effect of interfilm coupling can be obtained by studying the eigenvectors of the modes as a function of position in the multilayer. In our structure, it is sensible to separate the results for the two sublattices. We therefore define spin-wave amplitudes $\mathbf{a}_i$ for one sublattice and amplitudes $\mathbf{b}_i$ for the second sublattice within the film. The index i runs from 1 to N and labels pairs of adjacent sublattices:

$$\mathbf{a}_i=\mathbf{s}_{2i-1}, \tag{6}$$

$$\mathbf{b}_i=\mathbf{s}_{2i}. \tag{7}$$

In Fig. 5(a) we present the eigenvectors corresponding to the lowest frequency spin-wave modes of in Fig. 4 with no interfacial coupling between the two films ($H_{\mathrm{I}}=0$). Both a_x (solid lines) and b_x (dotted lines) are shown. It is immediately apparent that these mode profiles are very complicated. The modes contain both bulk and surface mode characteristics and it is difficult to extract the key features of the profiles. Furthermore there is no obvious symmetry about the midplane of the individual films as one might expect in the absence of interfacial coupling. This figure, however, does indicate that it might not be appropriate to use a long-wavelength approximation to solve for the spin motion. This will be of importance in the next section where we discuss effective-medium theories.

A simpler version of the mode profiles may be constructed which demonstrates the symmetry of the mode profiles with respect to the midplane of each individual film. As discussed in Ref. 26, the symmetry of the mode amplitudes with respect to the midplane of the film are only well defined in terms of the sum of the amplitudes on each sublattice. Therefore an average amplitude is defined for each pair of magnetic sublattices according to

$$\langle \mathbf{s}_i \rangle=(\mathbf{a}_i+\mathbf{b}_i)/2. \tag{8}$$

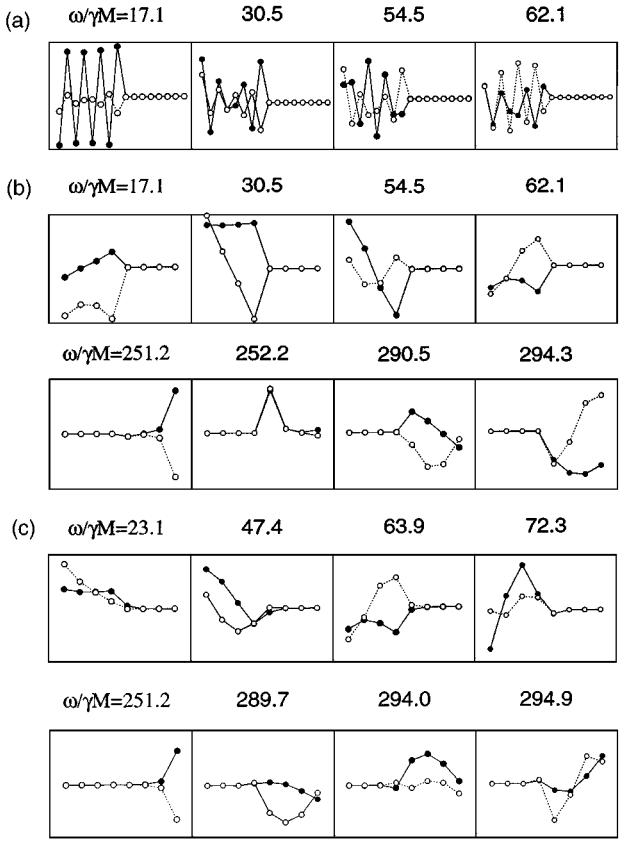

FIG. 5. Eigenvector solutions for the spin-wave modes as a function of position for two coupled films. The parameters are the same as in Fig. 4 with $H_I/M=0$ for (a) and (b). The eigenvectors are labeled according to frequency. In (a), the solid lines are the a_x and the dotted lines are the b_x for the low frequency modes in the bilayer. In (b), $\langle s_x\rangle=(a_x+b_x)/2$ is shown by the solid line. The dotted line in (b) is $\langle s_y\rangle$. The $\langle s_x\rangle$ and $\langle s_y\rangle$ for $H_I/M=100$ are shown in (c). The surface modes have the largest amplitude at the interface and are therefore strongly affected by pinning due to the interfilm coupling.

Note that the right and left eigenvectors are not equivalent because of the dipole terms in the equation of motion matrix. In our discussions of mode profiles, we present results for the right eigenvectors unless otherwise stated.

Transverse amplitudes $\langle s_x\rangle$ and $\langle s_y\rangle$ are shown in Fig. 5(b) as a function of position for the same two film multilayer of Fig. 5(a). Comparison of $\langle s_x\rangle$ (shown by the solid line) and a_x and b_x in (a) clearly demonstrate how symmetry about the midplane of each film is only well defined for the magnetization averaged over sublattice pairs.

Mode profiles with $H_I/M=100$ are shown in (c). The other parameters are the same as in (a) and (b). The solid lines in (c) are for $\langle s_x\rangle$ and the dotted lines are for $\langle s_y\rangle$. Comparison of (b) and (c) show how the interfilm coupling H_I affects the mode profiles, and consequently, the mode frequencies. The main point we wish to emphasize is that not all modes are affected equally by H_I. This can be seen in Fig. 4 and understood by reference to the profiles in Figs. 5(b) and 5(c). The modes most sensitive to H_I are identified as surface modes. This is particularly evident for the $\omega/\gamma M=252.2$ mode shown in (b) where $H_I=0$. This mode is strongly localized to the interface between the two antiferromagnets. [The strong localization for this film is due to the large H_a (Ref. 19)]. When interfacial exchange is turned on [as for Fig. 5(c)] we see a significant change in the mode profile with a corresponding increase in frequency.

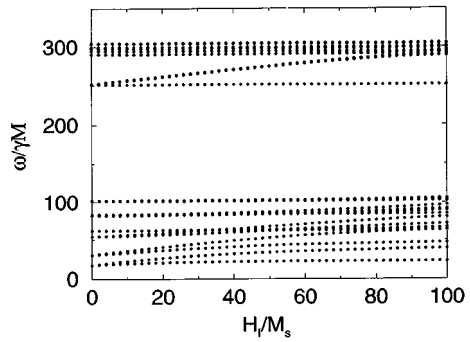

FIG. 6. Spin-wave frequencies as a function of interfilm exchange H_I for 12 coupled films. Each film has eight atomic layers. The parameters $H_e/M=100$, $H_u/M=1$, and $qa=0.002$ are the same for each film. As in Fig. 4, $H_a^I/M=200$ and $H_a^{II}/M=2$. The external field is $H_o/M=0.5$. The features are similar to the bilayer case of Fig. 4 with the difference that the interfilm coupling creates bands of nearly degenerate collective modes.

This sensitivity to H_I can be understood in terms of the interface exchange fields. When interfilm exchange coupling exists between two dissimilar materials, the outermost spins of one film at a resonance drive the outermost spins of the adjacent film away from their resonance. This pins the spins at the interfaces and increases the magnitude of the normal wave-vector component in a spin-wave mode. This in turn increases the exchange energy in the mode, driving it upwards in frequency. The greatest frequency increase occurs for surface modes with amplitudes localized to the interface between the two films. Pinning drives these modes up in frequency whereas the other surface modes, with amplitudes localized to the free surfaces, are not affected. This is what happens for the $\omega/\gamma M=251.2$ surface mode of film II. The corresponding mode amplitude in Fig. 5(b) show that this mode is strongly localized to the free surface where there is no exchange coupling. As a result, the mode frequency for this surface mode remains approximately unaffected.

Similar behavior is seen in Figs. 5(b) and 5(c) for the surface modes of film I where large changes in mode profiles near the interface are associated with significant changes in the frequency of the modes. The behavior of a multilayer with more than two films is essentially the same. The frequencies as a function of H_I are shown in Fig. 6 for a 12-film multilayer with six films of type I and six films of type II using parameters given above. Each film has eight atomic layers and an external field is applied in the z direction with magnitude $H_o/M=0.5$.

The structure is the same as that for the two-film example of Fig. 4 except that bands of modes form with increasing H_I. The interfilm coupling lifts the degeneracy of spin-wave modes from like films. The effect is not large, and thus narrow bands of ''collective'' excitations are created. The surface modes are again the most sensitive to interfilm exchange induced pinning. Note the complicated structure as a band of surface modes increase in frequency and pass through the other modes.

IV. ENTIRE-CELL EFFECTIVE-MEDIUM THEORY

The above theory is useful for finite multilayers provided the total number of atomic layers is not too large. For superlattices containing several hundred or more atomic layers, computational demands become too large and alternative approaches need to be found. One of the most useful approaches that reduce the complexity of the problem has been effective-medium theory.

Effective-medium theory provides a method for constructing magnetic-susceptibilities in a multilayer geometry that satisfy the Maxwell electromagnetic boundary conditions at each interface.[21–23] A key requirement in the conventional form of effective-medium theory is that the amplitude of the spin fluctuations associated with the excitation be constant across a unit cell of the multilayer. This is reasonably well approximated by the surface mode on multilayers composed of thin ferromagnetic films. As we have seen, this is not the case for antiferromagnetic thin films and multilayers.

In order to fully understand the nature of the various approximations involved, we now compare results for single thin films using different degrees of approximation within an effective-medium description. The first and simplest form considers a single microscopic unit cell of the antiferromagnet. The equations of motion then couple spins from each sublattice according to

$$(i\omega/\gamma)a_x-[H_o+H_a+H_u+H_e]a_y+H_eb_y=Sh_y^a, \quad (9)$$

$$[H_o+H_a+H_e]a_x+i\omega/\gamma a_y+H_eb_x=-Sh_x^a, \quad (10)$$

$$(i\omega/\gamma)b_x-[H_o+H_a+H_u+H_e]b_y+H_ea_y=-Sh_y^b, \quad (11)$$

$$[H_o+H_a+H_e]b_x+(i\omega/\gamma)b_y+H_ea_x=Sh_x^b. \quad (12)$$

These equations of motion differ from Eq. (2) in that the dipolar fields **h** are left unspecified. Note also that translational invariance in all directions has been assumed so that the amplitudes **a** and **b** are independent of position in the film.

The effective-medium approximation in this case consists of defining average fields according to

$$\langle \mathbf{m}\rangle=(\mathbf{a}+\mathbf{b})/2 \quad (13)$$

and

$$\langle \mathbf{h}\rangle=(\mathbf{h}^a+\mathbf{h}^b)/2 \quad (14)$$

with the requirement that the fields satisfy Maxwell's electromagnetic boundary conditions everywhere. This means that tangential **h** and normal **B** fields are continuous:

$$h_x^a=h_x^b \quad (15)$$

and

$$h_y^a+4\pi a_y=h_y^b+4\pi b_y\,. \quad (16)$$

These conditions together with Eqs. (9)–(12) allow one to define an effective susceptibility χ according to

$$\langle \mathbf{m}\rangle=\chi\langle \mathbf{h}\rangle. \quad (17)$$

Results for the components of the susceptibility are given in Ref. 23.

The susceptibilities defined this way work well for thick films but are clearly unable to describe the effects of surfaces. One way to include surface effects is to use thickness averaged effective fields in the equations of motion. This means, for example, that the exchange fields appearing in Eqs. (9)–(12) are multiplied by thickness-dependent weighting factors. The justification for this is the assumption of long-wavelength excitations. In this case, one might expect that all spins on a given sublattice essentially move together as if they are ''rigidly coupled.'' Such an approximation has been successfully employed in understanding the spin waves in Fe/Cr-type multilayers where ferromagnetic films which are weakly coupled through some spacer material.

We can obtain the weighting factors by a simple argument. Consider a film with $2N$ planes of spins. Each plane of spins is exchanged coupled to two planes, one above and one below, and therefore contributes $2J$ except for the one surface plane of sublattice A which is only coupled on one side. This plane therefore contributes just J. The total exchange energy of the spins on sublattice A is thus proportional to $(2N-1)J$. The average exchange field for sublattice A is then simply proportional to $(2N-1)J/N$. For example, Eq. (9) becomes

$$(i\omega/\gamma)a_x-[H_o+H_a+H_u+(f/2)H_e]a_y+(f/2)H_eb_y=Sh_y^a, \quad (18)$$

where $f=(2N-1)/N$. This procedure can be established more rigorously as well.

Since the surface anisotropy may be different from that of the bulk, one may also obtain thickness-dependent anisotropy terms in a similar manner. This approach is simple and improves the calculated values for the long-wavelength modes in thin films. Nonetheless, there is still considerable error in thin films as we shall see. The reason is that the long-wavelength assumption that all the spins on a given sublattice move rigidly together does not properly represent the dynamics of a thin-film antiferromagnet.

This can be seen by examining the eigenvectors calculated from the microscopic theory. Examination of the eigenvectors for the uncoupled films in Fig. 5 suggest that the approximation of a constant spin-wave amplitude does not apply to thin antiferromagnetic films. The small variation in mode amplitude across the film can involve a significant exchange energy. The frequencies of the resonance modes, for the multilayer of Fig. 5 for example, are only approximated to within 10% by the previous thickness weighted effective-medium theory. The error is reduced for multilayers constructed from thicker films because the frequencies move toward the bulk limits.

This result is somewhat counterintuitive in that effective-medium theory for surface modes on ferromagnetic multilayers is best for multilayer constructed from thin ferromagnetic films. The difference from the antiferromagnetic multilayer is that the surface mode amplitude is very nearly constant across a thin ferromagnetic film, and becomes more constant as the film is made thinner. From Fig. 5, we see that variations in the amplitude of the resonance mode in even a thin eight-layer antiferromagnetic film can be significant.

Variations of a component of the mode amplitude across the individual magnetic films does not mean that an effective-medium approximation cannot be applied. In order to use effective-medium theory in this situation it is instead necessary to relax the assumption that the surface mode can be described by position independent magnetic fields.

An accurate effective-medium theory can be constructed in the following way. The complete equations of motion are written for a single unit cell consisting of N_{I}-type I layers and N_{II}-type II layers. The total thickness of the unit cell is $N_{\mathrm{I}}+N_{\mathrm{II}}$. The limit of $q=0$ is taken so that there is no contribution from exchange interactions due to propagation in the plane of the film.

In material I, the equations of motion for $1<i<N_{\mathrm{I}}$ have the form:

$$(i\omega/\gamma)a_{i,x}-[H_o+H_a^{\mathrm{I}}+H_u^{\mathrm{I}}+2H_e^{\mathrm{I}}]a_{i,y}+H_e^{\mathrm{I}}b_{i,y}+H_e^{\mathrm{I}}b_{i-1,y} = S^{\mathrm{I}}h_{i,y}^a, \tag{19}$$

$$[H_o+H_a^{\mathrm{I}}+2H_e^{\mathrm{I}}]a_{i,x}+(i\omega/\gamma)a_{i,y}+H_e^{\mathrm{I}}b_{i,x}+H_e^{\mathrm{I}}b_{i-1,x} = -S^{\mathrm{I}}h_{i,x}^a, \tag{20}$$

$$(i\omega/\gamma)b_{i,x}-[H_o+H_a^{\mathrm{I}}+H_u^{\mathrm{I}}+2H_e^{\mathrm{I}}]b_{i,y}+H_e^{\mathrm{I}}a_{i,y}+H_e^{\mathrm{I}}a_{i+1,y} = -S^{\mathrm{I}}h_{i,y}^b, \tag{21}$$

$$[H_o+H_a^{\mathrm{I}}+2H_e^{\mathrm{I}}]b_{i,x}+(i\omega/\gamma)b_{i,y}+H_e^{\mathrm{I}}a_{i,x}+H_e^{\mathrm{I}}a_{i+1,x} = S^{\mathrm{I}}h_{i,x}^b. \tag{22}$$

Similar sets of equations are written for the spins in material II.

Periodic boundary conditions are used for the first layer so that $b_0=b_{N_{\mathrm{I}}}$ and $a_{N_{\mathrm{II}+1}}=a_1$. The equations of motion for $i=1$ and $i=N_{\mathrm{I}}$ are therefore

$$(i\omega/\gamma)a_{1,x}-[H_o+H_a^{\mathrm{I}}+H_u^{\mathrm{I}}+2H_e^{\mathrm{I}}]a_{1,y}+H_e^{\mathrm{I}}b_{1,y}+H_{\mathrm{I}}b_{N_{\mathrm{II}},y} = S^{\mathrm{I}}h_{1,y}^a, \tag{23}$$

$$[H_o+H_a^{\mathrm{I}}+2H_e^{\mathrm{I}}]a_{1,x}+(i\omega/\gamma)a_{1,y}+H_{\mathrm{I}}b_{i,x}+H_e^{\mathrm{I}}b_{N_{\mathrm{II}},x} = -S^{\mathrm{I}}h_{1,x}^a, \tag{24}$$

and

$$(i\omega/\gamma)b_{N_{\mathrm{I}},x}-[H_o+H_a^{\mathrm{I}}+H_u^{\mathrm{I}}+2H_e^{\mathrm{I}}]b_{N_{\mathrm{I}},y}+H_e^{\mathrm{I}}a_{N_{\mathrm{I}},y} +H_{\mathrm{I}}a_{N_{\mathrm{I}+1},y}=-S^{\mathrm{I}}h_{N_{\mathrm{I}},y}^b, \tag{25}$$

$$[H_o+H_a^{\mathrm{I}}+2H_e^{\mathrm{I}}]b_{N_{\mathrm{I}},x}+(i\omega/\gamma)b_{N_{\mathrm{I}},y}+H_e^{\mathrm{I}}a_{N_{\mathrm{I}},x}+H_{\mathrm{I}}a_{N_{\mathrm{I}+1},x} = S^{\mathrm{I}}h_{N_{\mathrm{I}},x}^b. \tag{26}$$

Analogous equations apply for the spins at $N_{\mathrm{I}+1}$ and $N_{\mathrm{I}+\mathrm{II}}$.

The effective susceptibility [defined in Eq. (17)] for a multilayer is constructed by forming average response functions from Eqs. (19)–(26). The averages are constructed in accordance with macroscopic electromagnetic theory as before by requiring the tangential components of the dipolar field **h** and normal components of the magnetic induction **B** to be continuous across interfaces. Instead of Eqs. (15) and (16), for the entire-cell method we require

$$h_{i,x}^a=h_{i,x}^b=C_x \tag{27}$$

and

$$h_{i,y}^a+4\pi a_{i,y}=h_{i,y}^b+4\pi b_{i,y}=C_y. \tag{28}$$

The amplitudes C_x and C_y are constant. This condition together with the equations of motion [Eqs. (19)–(26)] and Eqs. (27) and (28) form a set of $3(N_{\mathrm{I}}+N_{\mathrm{II}})+1$ coupled equations with unknown amplitudes **a**,**b** and arbitrary constants C_x and C_y.

With $N_{\mathrm{I}}+N_{\mathrm{II}}=N$, the average magnetization $\langle\mathbf{m}\rangle$ and average dipole field $\langle\mathbf{h}\rangle$ are

$$\langle\mathbf{m}\rangle=\frac{1}{N}\sum_i(\mathbf{a}_i+\mathbf{b}_i), \tag{29}$$

$$\langle\mathbf{h}\rangle=\frac{1}{N}\sum_i(\mathbf{h}_i^a+\mathbf{h}_i^b). \tag{30}$$

The susceptibilities $\chi_{\alpha\beta}$ can be determined numerically as follows. The sets of Eqs. (19)–(28) and (30) are solved at a given frequency ω to find **a**, **b** and $\langle\mathbf{h}\rangle$ as a function of C_x and C_y. The $\langle\mathbf{m}\rangle$ are constructed according to Eq. (29) above and values for the $\chi_{\alpha\beta}$ are found by from $\chi_{\alpha\beta}=\langle m_\alpha\rangle/\langle h_\beta\rangle$. For example, χ_{xy} is found this way by calculating the $\langle m_x\rangle$ as in Eq. (29) with $C_x=0$ and $C_y=1$. χ_{xx} is then found by repeating the calculation with $C_x=1$, allowing one to write

$$\chi_{xx}=(\langle m_x\rangle-\chi_{xy}\langle h_y\rangle)/\langle h_x\rangle. \tag{31}$$

From the computed values $\boldsymbol{\chi}$ we may obtain the permeability tensor given by $\mu=\mathbf{1}+4\pi\boldsymbol{\chi}$. For our geometry, this tensor takes the usual form for an anisotropic and gyrotropic material

$$\mu=\begin{pmatrix}\mu_{xx}&\mu_{xy}&0\\ \mu_{yx}&\mu_{yy}&0\\ 0&0&1\end{pmatrix}=\begin{pmatrix}\mu_1&i\mu_2&0\\ -i\mu_2&\mu_3&0\\ 0&0&1\end{pmatrix}. \tag{32}$$

In the absence of damping μ_{xx} and μ_{yy} are purely real and μ_{xy} is pure imaginary. We have included a small damping term in our calculations which makes all the permeabilities complex, but we continue to focus on the real parts of μ_{xx} and μ_{yy} and the imaginary part of μ_{xy}. The behavior of the individual components of the permeability as a function of frequency are shown in Fig. 7 for uncoupled antiferromagnetic films and in Fig. 8 for strongly coupled films. The examples are made using parameters from earlier examples ($H_u^{\mathrm{I}}/M=H_u^{\mathrm{II}}/M=1$, $H_a^{\mathrm{I}}/M=200$, $H_a^{\mathrm{II}}/M=2$, $H_e^{\mathrm{I}}/M=H_e^{\mathrm{II}}/M=100$, and $H_o/M=0.5$). The films are thin with $N_{\mathrm{I}}=N_{\mathrm{II}}=4$. The example in Fig. 7 has $H_{\mathrm{I}}/M=0$ and the example in Fig. 8 has $H_{\mathrm{I}}/M=100$.

Structure in the susceptibilities corresponds to different excitations. Note that the μ_{xx} and μ_{yy} measure the response of the superlattice to driving fields applied in different directions and therefore differ in their behavior. Both show a large response near the bottom of the spin-wave bands. The μ_{xy} component is nonzero in these examples because of the small applied field and has poles at frequencies where either μ_{xx} or μ_{yy} show a response.

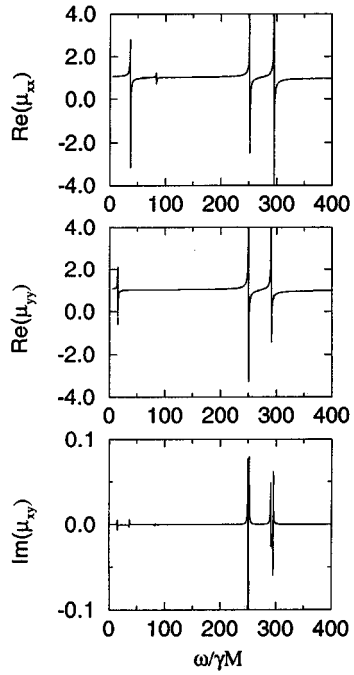

FIG. 7. Effective-medium susceptibilities for equal thickness films with $N_{\mathrm{I}}=N_{\mathrm{II}}=4$. The parameters are the same as in Fig. 6 with $H_{\mathrm{I}}=0$. The three unique components μ_{xx}, μ_{yy}, and μ_{xy} are shown as functions of frequency. The resonance frequencies of each film are very different, so that the peaks in the μ tensor fall in two separate sets.

The poles correspond to standing spin-wave excitations in the structure. The strongly coupled superlattice response shown in Fig. 8 has more structure than the uncoupled superlattice of Fig. 7. This is because the interfilm coupling lifts the degeneracy of modes from like films, as discussed already in reference to Fig. 6.

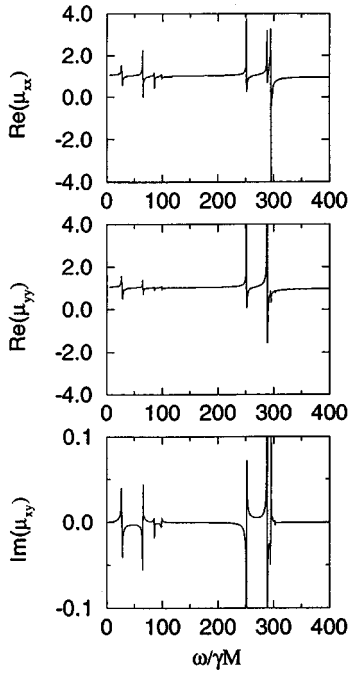

FIG. 8. Effective-medium susceptibilities for equal thickness films. Parameter values are the same as in Fig. 6 except $H_{\mathrm{I}}/M=100$. Note the appearance of more structure as the degeneracy between modes is removed by the interfilm exchange.

We note that the entire-cell effective-medium theory also provides information on the dipole strength of the standing waves as well as the long-wavelength resonant mode. For example in Fig. 7 we see a resonance in μ_{yy} near $\omega/\gamma M=16$ which is due to the long-wavelength resonant mode. A similar resonance (at a slightly different frequency) is seen in the ''rigid coupling'' effective-medium theory. However, the strong excitation in μ_{xx} near $\omega/\gamma M=37$ corresponds to a standing wave and cannot be obtained within conventional effective-medium theory. As a result, our entire-cell effective-medium theory should be more useful than conventional effective-medium theory in characterizing the infrared behavior for antiferromagnetic thin films and multilayers. The permeabilities calculated here can be used directly in standard electromagnetic formulations of reflectivity, for example. Although this will not be discussed further here, we do present an example of magnetostatic waves in what follows.

To further illustrate the differences between the different effective-medium approaches discussed above, we compare the frequencies of the magnetostatic spin waves calculated using different effective-medium susceptibilities to the frequencies calculated from the microscopic model. The effective-medium responses were found by solving the boundary condition problem for magnetostatic waves in a thin film. The essence of this calculation involves solving $\nabla\cdot\mathbf{B}=0$ together with $\nabla\times\mathbf{h}=0$ and applying boundary conditions on continuity of normal $\mathbf{B}$ and tangential $\mathbf{h}$ at the film surfaces. The end result is an implicit dispersion equation[27] for the frequency of long-wavelength magnetostatic spin waves in a film of thickness L:

$$q^2+2qq_y(\mu_{xx})\cot(q_yL)-q_y^2(\mu_{yy})^2-q_x^2\mu_{xy}^2=0, \quad (33)$$

where

$$q_y^2=(\mu_{xx})(q^2+q_x^2)/\mu_{xy}. \quad (34)$$

Frequencies that satisfy Eqs. (33) and (34) are listed in Tables I and II.

Table I contains the lowest magnetostatic mode frequencies for a single film calculated using the entire-cell effective-medium susceptibilities and the earlier rigid coupling effective-medium susceptibilities. The frequencies are shown for different film thicknesses and the parameters are the same as in Fig. 3 with $\mathbf{q}=0$. Both sets of susceptibilities give the same qualitative dependence on film thickness, but the frequencies differ considerably. The unit-cell frequencies agree to within 0.01% with the frequencies predicted by microscopic theory. Both methods of calculation lead to the correct bulk limit of 20.7 as the film becomes very thick, but the rigid coupling approximation clearly fails to correctly describe finite-size effects for thin films.

The entire-cell method also does quite well in describing the higher frequency spin-wave excitations, even in a multilayer. This is illustrated with spin-wave frequencies presented in Table II calculated using the entire-cell effective-medium susceptibility in Eqs. (33) and (34) and

TABLE I. Comparison of magnetostatic wave frequencies calculated with different effective-medium susceptibilities for a single thin film. The parameters are the same as in Fig. 3. Frequencies, $\omega/\gamma M$, calculated using the entire film as the unit cell and the rigid coupling approximation are shown in comparison to the bulk antiferromagnetic frequency as functions of the number of atomic layers (N) in the film. For reference, the bulk antiferromagnetic resonance frequency in these units is 20.7

N	Entire-cell	Rigid coupling
2	15.2	18.2
4	15.9	19.5
6	16.6	19.9
8	17.2	20.2
10	17.6	20.3
12	18.0	20.4
14	18.2	20.4
16	18.5	20.5
18	18.6	20.5
20	18.7	20.6

also with microscopic theory for a two-film unit-cell structure. The parameters are those used in Figs. 7 and 8 with $N_{\mathrm{I}}=N_{\mathrm{II}}=4$.

The eigenfrequencies found from the microscopic theory were calculated for a similar two-film multilayer with a total of eight atomic layers (and at $q=0$). The agreement between the models is best for zero interfilm coupling. The two methods also compare favorably in the limit of strong coupling although differences appear due to finite-size effects in the microscopic model (which does not assume periodic boundary conditions). Finally we note that the two models give converging results as the thickness and number of films are increased.

V. SUMMARY AND CONCLUSIONS

In this paper we have studied spin-wave modes in antiferromagnetic thin films and multilayers and provided a detailed comparison of different approximate methods of calculation. We consider easy-plane structures and use a microscopic theory which includes exchange, anisotropy, and dipolar fields to examine the severity of different effective-medium approximations. Our key results show how interface exchange coupling effects the frequencies of the spin-wave modes. We show that interface exchange can produce large frequency shifts for spin waves which have large amplitudes near the interfaces. These shifts can therefore be used to obtain accurate values for interfacial exchange in antiferromagnetic superlattices.

One way of obtaining spin-wave frequencies in antiferromagnets is through infrared reflectivity measurements. For this it is helpful to obtain an effective magnetic permeability tensor for the magnetic medium. This is often done within an effective-medium approach. We demonstrate that current effective-medium treatments are not accurate for spin waves in very thin films and in superlattices composed of thin films. The reason for this is that the usual long-wavelength assumptions used in conventional effective-medium theory break down for antiferromagnetic films. In addition, conventional effective-medium theory is not designed to obtain the shorter wavelength excitations (standing waves) found in thin films and superlattices. These standing spin waves can contribute significantly to response at infrared wavelengths.

TABLE II. Comparison of magnetostatic wave frequencies $\omega/\gamma M$ calculated with effective-medium susceptibilities and spin-wave frequencies from microscopic theory for $N_{\mathrm{I}}=N_{\mathrm{II}}=4$. The parameters are the same as those in Figs. 7 and 8.

$H_{\mathrm{I}}=0$		$H_{\mathrm{I}}/M=100$	
Eff. medium	Microscopic	Eff. medium	Microscopic
15.9	15.9	28.3	29.3
37.3	37.3	65.5	64.7
82.1	82.1	86.4	87.2
83.7	83.7	99.1	98.1
251.2	251.2	252.2	251.2
252.3	252.3	292.2	293.1
297.4	297.4	299.7	298.8
299.5	299.5	301.1	302.1

In view of these considerations, we have developed a modified effective-medium theory which is not dependent on a long-wavelength assumption. As a test of our results, we use our calculated permeabilities to obtain the frequencies of the spin-wave modes in a thin film. We find good agreement for all the modes, including the surface waves and the standing waves. The derived permeability tensor also gives information on the strength of the interaction between an external infrared beam and the magnetic medium. Our results indicate that some of the shorter wavelength standing waves show features in the permeability which are as large as that shown by the longer wavelength modes usually measured in infrared reflectivity. Note: a complementary approach dealing with similar issues was brought to our attention during the final preparation of this manuscript (Dumelow *et al.*, Ref. 28).

ACKNOWLEDGMENTS

This work was supported by US ARO Grant No. DAAH04-94-G-0253. R.E.C. was also supported by EPSRC.

*Permanent address: Dept. of Physics, Ohio State University, 174 West 18th Ave., Columbus, OH 43210.

†Permanent address: Dept. of Physics, University of Colorado at Colorado Springs, Colorado Springs, CO 80933-7150.

[1] A. S. Carriço and R. E. Camley, Phys. Rev. B **45**, 13 117 (1992).

[2] See, for example, the various estimates of J_1 given in Refs. 1, 19, and in R. W. Wang and D. L. Mills, Phys. Rev. B **46**, 11 681 (1992).

[3] J. A. Borchers, M. B. Salamon, R. W. Erwin, J. J. Rhine, R. R. Du, and C. P. Flynn, Phys. Rev. B **43**, 3123 (1991).

[4] C. A. Ramos, D. Lederman, A. R. King, and V. Jaccarino, Phys. Rev. Lett. **65**, 2913 (1990).

[5] D. M. Lind, S. D. Berry, G. Chern, H. Mathias, and L. R. Testardi, Phys. Rev. B **45**, 1838 (1992).
[6] J. A. Borchers, R. W. Erwin, S. D. Berry, D. M. Lind, J. F. Ankner, E. Lochner, D. A. Shaw, and D. Hilton, Phys. Rev. B **51**, 8276 (1995).
[7] T. Ambrose and C. L. Chien, Phys. Rev. Lett. **76**, 1743 (1996).
[8] J. F. Cochran, J. Rudd, W. B. Muir, B. Heinrich, and Z. Celinski, Phys. Rev. B **42**, 508 (1990).
[9] S. Demokritov, J. A. Wolff, and P. Grünberg, Europhys. Lett. **15**, 881 (1991).
[10] J. Faβbender, F. C. Nörtemann, R. L. Stamps, R. E. Camley, B. Hillebrands, G. Güntherodt, and S. S. P. Parkin, Phys. Rev. **46**, 5810 (1992).
[11] P. Kabos, C. E. Patton, M. O. Dima, D. B. Church, R. L. Stamps, and R. E. Camley, J. Appl. Phys. **75**, 3553 (1994).
[12] D. E. Brown, T. Dumelow, T. J. Parker, Kamsul Abraha, and D. R. Tilley, Phys. Rev. B **49**, 12 266 (1994).
[13] Kamsul Abraha, D. E. Brown, T. Dumelow, T. J. Parker, and D. R. Tilley, Phys. Rev. B **50**, 6808 (1994).
[14] M. R. F. Jensen, T. J. Parker, and D. R. Tilley, Phys. Rev. Lett. **75**, 3756 (1995).
[15] M. Lui, C. A. Ramos, A. R. King, and V. Jaccarino, J. Appl. Phys. **67**, 5518 (1990).
[16] L. L. Hinchey and D. L. Mills, Phys. Rev. B **33**, 3329 (1986); **34**, 1689 (1986).
[17] J. A. Borchers, M. J. Carey, R. W. Erwin, C. F. Majkrzak, and A. E. Berkowitz, Phys. Rev. Lett. **70**, 1878 (1993).
[18] R. W. Wang and D. L. Mills, Phys. Rev. B **50**, 3931 (1994); **53**, 2627 (1996).
[19] L. Trallori, P. Politi, A. Rettori, and M. G. Pini, J. Phys. Condens. Matter **7**, 7561 (1995).
[20] F. C. Nörtemann, R. L. Stamps, and R. E. Camley, Phys. Rev. B **47**, 11 910 (1993).
[21] N. S. Almeida and D. L. Mills, Phys. Rev. B **37**, 3400 (1988).
[22] N. Raj and D. R. Tilley, Phys. Rev. B **36**, 7003 (1987).
[23] R. L. Stamps, F. C. Nörtemann, R. E. Camley, and D. R. Tilley, Phys. Rev. B **48**, 15 740 (1993).
[24] M. C. Oliveros, N. S. Almeida, D. R. Tilley, J. Thomas, and R. E. Camley, J. Phys. Condens. Matter **4**, 8497 (1992).
[25] H. Benson and D. L. Mills, Phys. Rev. B **18**, 839 (1969).
[26] R. L. Stamps and R. E. Camley, Phys. Rev. B **35**, 1919 (1987).
[27] M. G. Cottam and D. R. Tilley, *Introduction to Surface and Superlattice Excitations* (Cambridge University Press, Cambridge, 1989).
[28] T. Dumelow and M. C. Oliveros, Phys. Rev. B (to be published).